

PHYSICAL MESOMECHANICS OF QUASI-VISCOUS FAILURE: THEORY AND EXPERIMENT

V.E. Egorushkin, V.E. Panin, A.V. Panin
Institute of Strength Physics and Materials Science SB RAS, 634021, Tomsk, Russia

ABSTRACT

The new approach to the development of criteria of quasiductile fracture is proposed based on the theory of nonlinear waves of localized inelastic deformation. It can be applied to consideration of quasiductile fracture of materials where the dislocation contribution to fracture can be disregarded (nanomaterials, surface hardened solids, thin films etc.).

1. THEORY OF NONLINEAR WAVES OF INELASTIC DEFORMATION

For dimensionless values of flow J and density α of linear defects (discontinuities of displacement vector u) in crystal the nonlinear wave equations have the form [1, 2]:

$$\frac{1}{c^2} \frac{\partial^2 J_a^\mu}{\partial t^2} - \frac{\partial^2 J_a^\mu}{\partial x_\nu^2} = \frac{\partial}{\partial t} \left\{ \frac{\partial \ln u_\alpha(x,t)}{\partial x_\mu} - \frac{1}{E} \frac{\partial \ln u_\beta}{\partial x_\nu} C_{\alpha\beta}^{\mu\nu} - \frac{1}{E} P_\nu^\beta C_{\alpha\beta}^{\mu\nu} \right\} \quad (1)$$

$$\frac{1}{c^2} \frac{\partial^2 \alpha_a^\mu}{\partial t^2} - \frac{\partial^2 \alpha_a^\mu}{\partial x_\nu^2} = \varepsilon_{\mu\alpha\sigma} \left\{ \frac{\partial^2 \ln u_\beta(x,t)}{\partial x_\chi \partial x_\nu} C_{\alpha\beta}^{\sigma\nu} - \frac{\partial P_\nu^\beta}{\partial x_\chi} C_{\alpha\beta}^{\sigma\nu} \right\} \frac{1}{E} \quad (2)$$

under the condition of compatibility for the sources

$$\frac{\partial N_\mu}{\partial t} + \varepsilon_{lm} \frac{\partial M_m}{\partial x_l} = 0,$$

where M is the right-hand part of eqn (1), N is the right-hand part of eqn (2), $u(x,t)$ are quasielastic displacements. In determining these displacements, it is useful to take into account the presence of the initial volume density of dislocations, viscosity and thermal expansion.

If L is the length and 2δ is the width of localised deformation region, than in the local area $r < L$ the flow equation has the form

$$\vec{J} = \frac{b_1 - b_2}{4\pi} \chi(s,t) \left(\ln \frac{2L}{r} - 1 \right) - \nabla f, \quad (3)$$

where \vec{b} is the vector of the binormal in the local coordinate system, \vec{n} is the normal, \vec{t} is the tangent, χ is the variation of the curvature of the region (variation of the curvature of the axis of the region) determined by the external load, s is the actual value of the length of the region, b_1, b_2 are the moduli of the "Burgers vector" of the volume translational and near-surface rotational incompatibility, respectively, ∇f is the gradient part of the flow, determined by secondary sources.

In the absence of ∇f the plastic strain rate is directed along the binormal, which depends on the actual value of the coordinate and time, to the side of the origin of the coordinates ($\nu = -\vec{J}$), is proportional to the curvature, the difference $(b_1 - b_2)$ and decreases in terms of the modulus with an increase of r at $r < L$ in accordance with the logarithmic law and the law $1/r^3$

at $r > L$. These equations indicate that as the length of the deformed region L decreases, the depth of propagation of the flow also decreases and the transverse spatial dimensions of propagation of plastic deformation become smaller (as in the effect of hardening the material by small particles).

The second effect is associated with strain localisation in the presence of an interphase boundary and subsurface misorientation. In this case, $b_2 \neq 0$ and the difference $(b_1 - b_2)$ may change the sign in some region in the vicinity of the boundary. Owing to the fact that in the vicinity of the boundary and at a distance from the boundary it is directed towards it, region of superimposition of the strain are possible when the effect of strain localisation in the vicinity of the interphase boundary or formation of subboundaries, may take place. The localisation effect may also occur as a result of compensation of the first and second term in the right-hand part eqn (3).

The spatial-time variations of the shape $E(s, t)$ during the deformation process (the process of change of shape) of the area, which is limited by length L and transverse dimensions may be determined from the equation

$$\vec{J} = \frac{\partial E(s, t)}{\partial t}, \quad (4)$$

where s – current value of length along the area.

Using the expression for \vec{J} and carrying out the substitution $t' \rightarrow t \frac{(b_1 - b_2)}{4\pi} \left(\ln \frac{2L}{r} - 1 \right)$ we obtain

$$\frac{\partial E(s, t)}{\partial t} = \chi \bar{b} - \frac{4\pi}{(b_1 - b_2) \left(\ln \frac{2L}{r} - 1 \right)} \nabla f. \quad (5)$$

In the absence of ∇f (or if ∇f has the same direction as \bar{b}), solving eqn (5), together with the equation $\frac{\partial \bar{E}}{\partial s} = \bar{t}$ and the Frene equations, it may be shown that the variation of the shape of the examined region is determined by the expressions:

$$E_x(s, t) = -\frac{2}{\beta(v^2 + 1)} \left\{ \sec h 2\beta(s + 4vt) \sin 2\beta(s + 4vt) - \sec h 8\beta vt \sin 8\beta vt \right\}, \quad (6)$$

$$E_y(s, t) = -\frac{2}{\beta(v^2 + 1)} \left\{ \sec h 2\beta(s + 4vt) \cos 2\beta(s + 4vt) - \sec h 8\beta vt \cos 8\beta vt \right\}, \quad (7)$$

$$E_z(s, t) = s - \frac{2}{\beta(v^2 + 1)} \left\{ th 2\beta(s + 4vt) - th 8\beta vt \right\}, \quad (8)$$

where $v = -\frac{\nu}{\beta}$.

The expressions (6-8) represent one of possible types of inelastic strain waves. They determine the variation of the shape of the region whose axis is a spiral curve with constant torsion $\tau = -2\nu$, equal to half the speed (-4ν) of displacement of the curve along the region with the curvature

$$\chi(s, t) = 4\beta \sec h[2\beta(s + 4vt)], \quad (9)$$

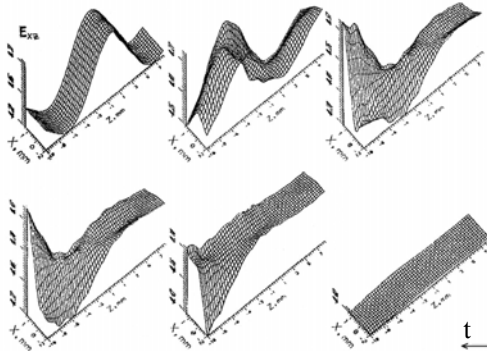


Figure 1: Development of deformation E_{xz} with time

χ can be measured in experiments and its value is equal to χ_e . Consequently, for v we

obtain (taking into account $t' = t \frac{b_1}{4\pi} \left(\ln \frac{2L}{r} - 1 \right)$)

$$v = \frac{\pi}{b_1 \ln \left(\frac{2L}{r} - 1 \right) t} \left\{ \frac{1}{2\beta} \text{Arc sec h} \frac{\chi_e}{4\beta} - z \right\}. \quad (10)$$

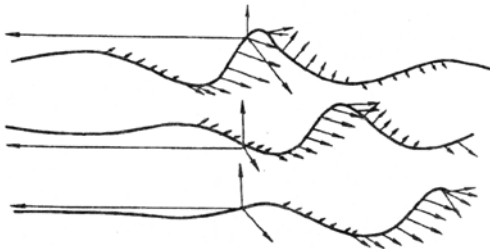


Figure 2: Variation of the form and rate of inelastic strain with time

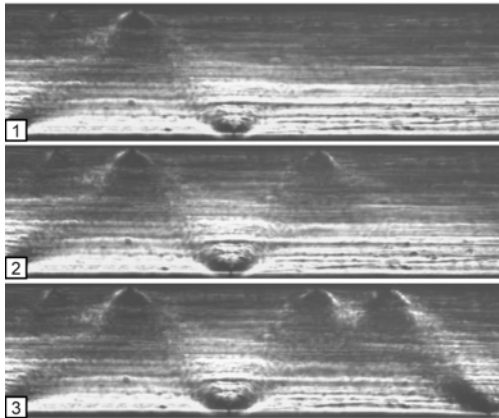


Figure 3: Propagation of a macroscopic localized-deformation band in the bulk of an ion-nitrided specimen as observed from lateral face. $\times 15$ [3]

decreasing from the maximum value 4β at the point $s = -4vt$ to 0 at $s \rightarrow \pm\infty$. This loop of spiral motion travels along the region with the speed $(-4v)$. The order of the length of displacement is approximately χ_{\max} .

Development of deformation component E_{xz} with the time is shown in Fig. 1. It is clear that the shape changes is realized by the wave of localized inelastic deformation.

The speed of displacement of the shape across the specimen can be determined easily from eqn (9) if it is assumed that

The variation of the inelastic strain rate with the time is shown in Fig. 2. The arrows indicate the magnitude and the direction of the inelastic strain rate in the vicinity of its axis. The strain rate is polarised perpendicularly in relation to the wave of the shape change, moving along the region. The variation of the direction of the rate along the curve is determined by the rotation of the vector of the binormal \vec{b} during the displacement of the local system of coordinates along s and with the variation of curvature. Fig. 2 shows that the maximum variation of the direction of the rate takes place in the region of "inflections" along the strain axis. In the area which the strain leaves the inelastic strain rate is equal to 0.

The theory of nonlinear waves of localized inelastic deformation is developed for loading of a solid with weak dissipation. Therefore such nonlinear waves can be experimentally revealed in solids where the dislocation contribution to deformation and fracture can be disregarded. First of all this is inherent in deformation of nanomaterials (both bulk nanomaterials and materials with

nanostructured surface layers), surface hardened solids, thin films etc. An example of the nonlinear wave of localized deformation is shown in Fig. 3 [3].

The face sides of a flat steel specimen were strengthened by ion nitriding. Therefore plastic flow by dislocation motion was suppressed. At the lateral sides of the flat specimen it can be seen the propagation of macroshear in the form of a spiral along the conjugate directions of τ_{\max} . It is discovered the alternating extrusion/intrusion zones in the vertexes of trihedral prisms formed by conjugate macroshears. Similar surface nonlinear waves are observed within nanostructured surface layers of low carbon steel and polycrystalline titanium [4].

The stage of necking is also related to suppression of dislocation motion. The development of nonlinear waves of localized inelastic deformation at necking stage governs a specimen fracture. Fracture criteria will be further considered.

2. THE WAVE MODEL AND CRITERIA OF QUASIDUCTILE FRACTURE

On the basis of the previously described wave nature of propagation of localized inelastic deformation it may be asserted that the necessary condition for quasiductile fracture is that the material must reach a state in which propagation of localized plastic deformation under loading is no longer possible. Since fracture takes place with the aid of corresponding stresses (sufficient conditions), the “arrest” of inelastic deformation is a prerequisite for fracture, and this state of the material may be regarded as the prefracture state (necessary condition already exist but sufficient conditions are not yet present). The model of achieving such a state may be based on the determined wave pattern of localized plastic strain, where the prefracture state may form because of the following reasons:

1. Loading cannot be accommodated by the variation of the local curvature of the deformed region (greatly hardened material, boundary, etc.) since plastic strain is not formed. In this case, brittle fracture is not associated with propagation of plastic deformation.
2. The variation of the curvature of the locally deformed region (boundary) in loading cannot be accommodated by the plastic flow \bar{J} propagating along the specimen (primary slip).
3. The plastic flow \bar{J} and the curvature cannot be accommodated by the wave of the shape variation (shape solution) across the specimen, i.e. the velocity of the shape solution tends to 0 (torsion $\tau \rightarrow 0$).
4. Mass transfer by the shape soliton cannot be accommodated by rotation of the grain (rotation of the deformed region).
5. Rotation of the grain (rotation of the region) cannot be accommodated by the boundaries of adjacent grains.

Since the curvature χ , determined by external loading, can be approximated by

$\chi \sim \frac{4\sigma_{zz}}{\delta E} (x \sim \delta)$, then according to the condition 2 and eqn (3), we have a criterion for the

transfer of the material to the prefracture state ($\nabla f \rightarrow 0$) in the vicinity of the axis of the deformed region

$$(\bar{J}\bar{b}) \frac{\pi E \delta}{(b_1 - b_2) \ln(2L/r - 1)} < \sigma_{zz}, \quad (11)$$

and away from the axis

$$(\bar{J}\bar{b}) \frac{3\pi E}{b_1} \left(\frac{r}{L}\right)^3 \delta < \sigma_{zz}. \quad (12)$$

At this moment and in the area where σ_{zz} reaches the critical value, the material fails by quasiductile fracture. If the actual \bar{J} is directed along the binormal \bar{b} , then eqn (11) and eqn

(12) include $|\bar{J}|$, and if the plastic flow is weak or plastic regions are very narrow and along, the material is already in the prefracture state at low stresses σ_{zz} . This also takes place when $\bar{J} \perp \bar{b}$, i.e. primary slip is realized inside the very plastically deformed region (boundary).

Conversely, if the plastic region is wide, and also at high E , the prefracture state occurs at high σ_{zz} . It should be mentioned that, in this case, the prefracture state is determined by the possibility of local bending of the deformed region and, consequently, the stresses σ_{zz} are fracturing. If the critical values of σ_{zz} are evaluated using $\sigma_{zz} \sim 9(1 + \sigma)/E$, then in eqn (11) and eqn (12) we can include only the Poisson coefficient.

Thus, under condition 2, a large service life reserve will be shown by the material with a high Young's modulus, strong plastic flows and large transverse dimensions of plastically deformed regions.

In case 3, the tendency of τ to 0 will be achieved in the following manner. The conditions imposed on strains at the boundaries of the deformed region should be such that

$$E_x(L) = E_x(-L), E_y(L) = E_y(-L), E_z(L) = E_z(-L). \quad (13)$$

This means that because of some circumstances, the strains at both ends of the region (boundary) are identical or the region is closed. The conditions eqn (13) show that $\tau = 0$ and the equations for the maximum curvature $\text{th}2\beta L = \beta L$ or $\beta \sim 1/L$ ($\chi_{\max} \sim 4/L$).

This case will be considered in special presentation "Mesoscopic levels of plastic flow within surface layers of polycrystals and their fatigue fracture under cyclic bending".

Experimental verification of the condition 2 for quasiductile fracture is illustrated in Fig. 4 for tension of nanostructured α -Fe [5]. The fragmented nanoband structure of α -Fe suppress dislocation motion and plastic flow $\bar{J} = 0$ along the specimen. Macrostress concentrators at the boundary between grip section of the specimen and its gauge length generate the macrobands of localized deformation in the form of a cross. Local curvature within



Figure 4: Optical images of the surface of the armco-iron specimen subjected to equal-channel angular pressing with subsequent annealing at 623 K, $\epsilon=7\%$ [5]

the cross of macrobands is not accommodated by plastic flow \bar{J} in the specimen gauge length. It causes the origination of a crack within the macrobands as an accommodation rotation mode. Specimen fracture develops being characterized by very low ductility.

Special annealing allows one to transform the fragmented nanoband structure of α -Fe to equiaxial submicrocrystalline substructure which is characterized by the condition $\bar{J} \neq 0$ along the gauge length of a specimen. Specimen ductility increases.

The condition 4 of quasiductile fracture is valid for all materials where necking stage occurs before fracture. In the general case two conjugate macrobands self-organized by the scheme of a cross develop within a specimen in the course of necking.

It does not always happen that one can manage to reveal macrobands of localized deformation in the neck in ordinary polycrystalline specimens under tension. The microscale dislocation deformation smears the macrobands, causing them to be weakly pronounced.

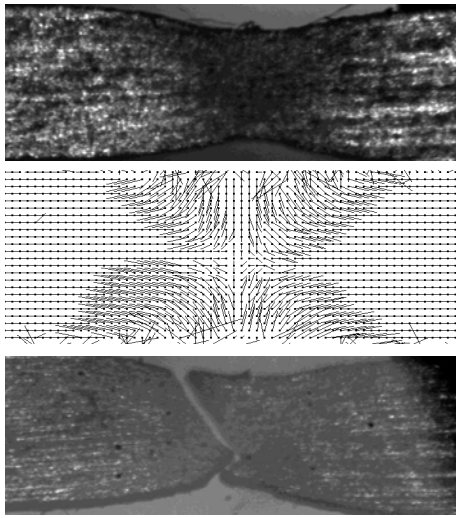


Figure 5: Formation of a neck and the character of fracture of a cold-rolled Ti specimen with a nanocrystalline surface structure under tension: an optical image of the specimen surface (a); the displacement vector field at the nanocrystalline surface (b); the character of fracture of the specimen (c); $\varepsilon = 17\%$. $\times 15$ [4]

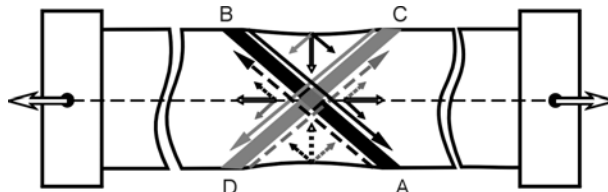


Figure 6: Schematic representation of shear accommodation in interaction of localized deformation macrobands in the form of a cross

However, if we retard the dislocation deformation, e.g., by forming a submicrocrystalline structure or a nanostructure at the surface or in the material bulk, the genesis of macrobands and the wave character of their evolution can clearly be defined in the displacement vector field on the descending portion of the “stress – strain” curve (Fig. 5). The scheme of the cross of self-conjugate macrobands (Fig. 5) is shown in Fig. 6. The specimen elongates mainly due to shears inside the macrobands accompanied by local curvature. In the bulk of the trihedral prisms AOD and BOC between intersecting localized macrobands displacement vectors are directed inside the specimen. In other words the trihedral prisms are indented into the bulk of the tensile specimen. This indentation is accompanied by material mesofragmentation as an accommodation rotation mode. At certain strain degree mesofragmentation within the neck is

stopped due to work-hardening. Mass transfer by the soliton of shape variation within the macroband cross cannot be accommodated by rotations in the areas AOD and BOC . There arises crack along BOD and the specimen fails (Fig. 5(c)).

REFERENCES

1. V. E. Egorushkin, Dynamics of plastic deformation. Localized inelastic strain waves in solids. in *Physical Mesomechanics of Heterogeneous Media and Computer-Aided Design of Materials*, Ed. by V.E. Panin, Cambridge International Science Publishing, Cambridge (1998) 41
2. V. E. Egorushkin. Dynamics of plastic deformation. Waves of localised plastic deformation in solids. // *Izv. Vuz. Fizika.* – 1992. – No. 4. – P 19.
3. N.A. Antipina, V.E. Panin, A.I. Slosman, B.B. Ovechkin. Switching waves of macroscopic localized deformation bands in tensile ion-nitrided specimens. // *Physical mesomechanics.* – 2000. – V.3. – No. 3. – P. 37-41.
4. A.V. Panin, V.A. Klimenov, Yu.I. Pochivalov, A.A. Son, M.S. Kazachenok. The effect of ultrasonic treatment on the mechanical behavior of titanium and steel specimens. // *Theoretical and Applied Fracture Mechanics.* – 41. – 1-3. – 2004. –P. 163-172.
5. A.V. Panin, A.A. Son, Yu.F. Ivanov, V.I. Kopylov. Features of localization and stages of plastic deformation of submicrocrystalline armco-iron with banded fragmented substructure. // *Physical mesomechanics.* – 2004. – V.7. – No. 3. – P. 5-16.